Steel and Composite Structures, *Vol. 34, No. 1 (2020) 155-170*
DOI: https://doi.org/10.12989/scs.2020.34.1.155

Identification of the most influencing parameters on the properties of corroded concrete beams using an Adaptive Neuro-Fuzzy Inference System (ANFIS)

Mahdi Shariati[1,2a], Mohammad Saeed Mafipour[3b], James H. Haido[4c], Salim T. Yousif[5d], Ali Toghroli[6e], Nguyen Thoi Trung[1,2f] and Ali Shariati*[6]

[1]Division of Computational Mathematics and Engineering, Institute for Computational Science, Ton Duc Thang University, Ho Chi Minh City, Vietnam
[2]Faculty of Civil Engineering, Ton Duc Thang University, Ho Chi Minh City, Vietnam
[3]School of Civil Engineering, College of Engineering, University of Tehran,Tehran, Iran
[4]Department of Civil Engineering, College of Engineering, University of Duhok, Kurdistan Region, Iraq
[5]Department of Civil Engineering, Al-Qalam University College, Kirkuk, Iraq
[6]Institute of Research and Development, Duy Tan University, Da Nang 550000, Viet Nam

(*Received March 25, 2019, Revised July 7, 2019, Accepted September 15, 2019*)

Abstract. Different parameters potentially affect the properties of corroded reinforced concrete beams. However, the high number of these parameters and their dependence cause that the effectiveness of the parameters could not be simply identified. In this study, an adaptive neuro-fuzzy inference system (ANFIS) was employed to determine the most influencing parameters on the properties of the corrosion-damaged reinforced concrete beams. 207 ANFIS models were developed to analyze the collected data from 107 reinforced concrete (RC) beams. The impact of 23 input parameters on nine output factors was investigated. The results of the paper showed the order of influence of each input parameter on the outputs and revealed that the input parameters regarding the uncorroded properties of concrete beams are the most influencing factors on the corresponding corroded properties of the beams.

Keywords: Adaptive Neuro-Fuzzy Inference System; system identification; corrosion; reinforced concrete beams

1. Introduction

Concrete is widely used as a constructional material across the world. The deterioration of the reinforced concrete members mainly results from the corrosion of steel rebar. Consequently, the service life of these structures decreases remarkably (Imam *et al.* 2015, Lu *et al.* 2017). Steel bars corrosion due to chloride effect is regarded as the significant deterioration problem, especially with using water in concrete batching, exposure of concrete to direct or indirect marine water, deicing with salts in cold climate areas, and concrete aggregate in saline contamination (Coronelli *et al.* 2004, Ma *et al.* 2014, Altoubat *et al.* 2016, Imam *et al.* 2016, Song *et al.* 2019). The penetration of chloride ion into concrete structures from the environment results in changing the chemistry of the solution of the concrete pore which leads to breakdown the passive protection layer on the steel surface in the alkaline conditions, resulting in a reduction of the cross-sectional area of steel bars and the volumetric increase of generated corroded parts (Fernandez *et al.* 2019).

The expansion of corroded materials volume leads to spilling and cracking of concrete cover, and with no resuscitation or retrofitting, the unexpected failure due to the reduction in cross-sectional area of steel bars can be produced, and then a reduction in loading capacity of the concrete member can occur (Broomfield 1997, Berto *et al.* 2009, Bossio *et al.* 2015, Bossio *et al.* 2017, Bossio *et al.* 2018).

Numerous analytical, numerical, and experimental studies have been conducted in the last three decades to investigate the behavior of concrete members with corroded reinforcement bars. The laboratory investigations were dealt with the capacity of structural members, bonding between corroded steel and concrete, cracking pattern of concrete elements, and strength of corroded steel bars (Cabrera 1996, Huang *et al.* 1997, Rodriguez *et al.* 1997, Sen *et al.* 1999, Wei-liang *et al.* 2001, Shannag *et al.* 2006, Azad *et al.* 2007, Torres-Acosta *et al.* 2007, Vidal *et al.* 2007, Berto *et al.* 2008, Wang 2008, Cavaco 2009, Kallias *et al.* 2010, Castel

*Corresponding author, Ph.D.
E-mail: alishariati@duytan.edu.vn
[a]Ph.D.
E-mail: shariati@tdtu.edu.vn
[b]Ms.C.
E-mail: m.saeed.mafipur@ut.ac.ir
[c]Ph.D.
E-mail: james.haido@uod.ac.ir
[d]Ph.D.
E-mail: dcivil443@yahoo.com
[e]Ph.D.
E-mail: alitoghroli@duytan.edu.vn
[f]Ph.D.
E-mail: nguyenthotrung@tdtu.edu.vn

http://www.techno-press.org/?journal=scs&subpage=6
ISSN: 1229-9367 (Print), 1598-6233 (Online)

et al. 2011, Khan *et al.* 2011, Oyado *et al.* 2011, Shariati *et al.* 2011a, Yamamoto *et al.* 2011, Imperatore *et al.* 2012, Zhu *et al.* 2014, Shetty *et al.* 2015, Kim *et al.* 2016, Maia *et al.* 2017, Paul *et al.* 2017, Yan *et al.* 2017, Zhou *et al.* 2019).

The prediction of the flexural capacity of reinforced concrete members has been the focus of recent researches by numerical and analytical methods. In a research, (Cabrera 1996) derived numerical models based on laboratory records, which relate the cracking or bond strength loss of concrete element to corrosion rate. In 1997, the conventional models in the Euro Code were used by (Rodriguez *et al.* 1997) to estimate the shear and flexural moment capacities of corroded concrete members. In another investigation, (Azad *et al.* 2007) used a regression analysis technique on the experimental data to find the residual strength of corroded reinforced concrete beam samples considering the reduced cross-sectional area of corroded steel bars. An empirical equation was proposed by (Ou *et al.* 2012) to produce the performance of large scale concrete beams under corrosion. It was concluded that analytical and experimental results have a good agreement with each other.

A research by (Mohammed *et al.* 2018) developed a simplified nonlinear finite element procedure based on nonlinear sectional analysis and material testing to investigate the structural response and residual strengths of slab on columns subjected to reinforced corrosion in addition to external forces. Various levels of material, geometrical, and bond damage have been taken into account as a result of reinforcement corrosion. The validity of this model has been verified by comparing the outcomes with analytical and experimental data for previous works. It was demonstrated that the critical design sections for a column or beam after corrosion damage do not necessarily remain critical for structural estimation. In 2017, (Paul and Van Zijl 2017) studied the cracking pattern of reinforced mortar beams in loading and unloading states under the effect of accelerated chloride corrosion. The pitting depth of corrosion, yield force, and loss of mass were recorded concerning corrosion rate. It was proved that the free chloride at steel surface level and crack spacing are best correlated to the damage of specimens due to the corrosion. A finite element modeling has been provided by (Shetty *et al.* 2015) to simulate the detrimental effect of corrosion on the bond behavior of concrete beams. Four levels of corrosion of 2.5, 5, 7.5, and 10% have been adopted in this modeling in ANSYS using Solid65 elements for concrete and Link8 elements for steel bars. The simulation yields 3% and 2.4% in bond strength reduction at the initial and ending of the slip by increasing the percentage of corrosion levels.

In a research (Lu *et al.* 2017) investigated the impact resistance of corroded reinforced concrete beams in falling weight experiments with considering accelerated deterioration. The relationship between impact resistance of beams and degree of deterioration has been formulated. Rebar corrosion was simulated by finite element with focusing on the ratio of mass loss of steel.

A reasonable agreement has been observed between numerical and experimental outputs. Fatigue behavior of corroded concrete beams was examined experimentally and analytically by (Song *et al.* 2019). Seven samples for the beams were tested, and an analytical fatigue model was applied to assess fatigue performance of the corroded reinforced concrete members.

The validation process was performed for the analytical model with the experimental data. Later, the model was extended to understand the influence of the corrosion pit geometry and corrosion degree at fatigue load level on the beam response. The authors found that there is a remarkable injurious effect on the fatigue behavior of the beams due to loss of steel bars area, stress concentration, and minimized bonding at the concrete-steel interface. Shear capacity of the corroded reinforced concrete beams has been investigated experimentally by (Imam and Azad 2016). Corrosion of steel bars was induced in acceleration produced by impressed current. It was found that the reduction in shear strength is attributed to cracking of concrete cover for the stirrups due to bars corrosion and decreasing in the area of the corroded shear bars. The experimental records were compared with the outputs of ACI code 318-08 (Committee *et al.* 2008) which was an analytical method, and suitable matching was observed between them.

Although composite beams and floor systems rarely encounter chloride attacks, the effect of corrosion is always a potential risk to them. On the other hand, the sensitivity of concrete against corrosion has been indicated by several studies; hence, the use of novel approaches to reduce the corrosion danger should be considered. Also, corroded concrete has different mechanical properties compared to intact concrete; therefore, in order to recognize the mechanical properties' quality of the corroded concrete, further studies are required (Shariati *et al.* 2010, Shariati *et al.* 2011b, Shariati *et al.* 2012b, Shariati *et al.* 2012a, Shariati *et al.* 2012d, Shariati *et al.* 2012c, Shariati 2013, Shariati *et al.* 2013, Shariati *et al.* 2014a, Shariati *et al.* 2014b, Khorramian *et al.* 2015, Shariati *et al.* 2015, Khorramian *et al.* 2016, Shahabi *et al.* 2016a, Shahabi *et al.* 2016b, Shariati *et al.* 2016, Tahmasbi *et al.* 2016, Khorramian *et al.* 2017, Shariati *et al.* 2017, Hosseinpour *et al.* 2018, Nasrollahi *et al.* 2018, Wei *et al.* 2018, Davoodnabi *et al.* 2019).

Since artificial intelligence algorithms have been proved to be useful in engineering applications, the development of different numerical and soft computing approaches is an absolute necessity for precise evaluation of the critical parameters in engineering; hence, the generated algorithms and accurate predictions would be achieved. Although the mechanical performances of some specific corroded concrete have been investigated through experimental results, other corroded concretes with different damages should be evaluated. Therefore, these mechanical properties could be obtained along with the conducted artificial intelligence algorithms on precursor experimental data (Hamidian *et al.* 2012, Sinaei *et al.* 2012, Hamdia *et al.* 2015, Mohammadhassani *et al.* 2015, Toghroli 2015, Mansouri *et al.* 2016, Thang *et al.* 2016, Toghroli *et al.* 2016, Khorami *et al.* 2017, Tai *et al.* 2017, Sadeghipour Chahnasir *et al.* 2018, Sari *et al.* 2018, Toghroli *et al.* 2018a,

Table 1 Input parameters

Input No.	Input Name	Input No.	Input Name
Input 1	Span length (mm)	Input 13	Spacing A'_s (mm)
Input 2	Width (mm)	Input 14	Compressive strain at f'_c uncorroded
Input 3	Depth (mm)	Input 15	Crushing strain uncorroded
Input 4	Age (day)	Input 16	Tensile strain at f_t uncorroded
Input 5	f'_c uncorroded (MPa)	Input 17	f_y uncorroded (MPa)
Input 6	f_t uncorroded (MPa)	Input 18	f'_y uncorroded (MPa)
Input 7	E_c uncorroded (MPa)	Input 19	Number of beams per span
Input 8	P_u corroded (kN)	Input 20	Number of decks per span
Input 9	Delta corroded (mm)	Input 21	Number of spans
Input 10	A_s uncorroded (mm^2)	Input 22	f_u uncorroded (MPa)
Input 11	A'_s uncorroded (mm^2)	Input 23	f'_u uncorroded (MPa)
Input 12	Spacing A_s (mm)		

Toghroli *et al.* 2018b, Milovancevic *et al.* 2019, Katebi *et al.* 2019, Mansouri *et al.* 2019, Shariati *et al.* 2019d, Shariati *et al.* 2019e, Trung *et al.* 2019, Xu *et al.* 2019).

Moreover, the beam to column composite joints and composite beams which perform as the most crucial structural elements should remain intact during the serviceability. Also, In order to maintain safety, central members should be serviceable in any condition. In this case, it is essential to carry out various approaches to evaluate the mechanical properties of the corroded concrete and obtain the important design features (Arabnejad Khanouki *et al.* 2011, Sinaei *et al.* 2011, Mohammadhassani *et al.* 2014a, Mohammadhassani *et al.* 2014b, Arabnejad Khanouki *et al.* 2016, Shah *et al.* 2016, Heydari *et al.* 2018, Ismail *et al.* 2018, Luo *et al.* 2019, Shi *et al.* 2019, Xie *et al.* 2019). Besides, the surface of roads and sidewalks are directly subjected to corrosion hazards. Hence, the corrosion probability has always been a potential threat to the pavements. Thereby, the pavements which have been produced by pervious concrete should be resistant to chloride penetrations and vehicle effects (Toghroli *et al.* 2017, Toghroli *et al.* 2018b, Li *et al.* 2019, Milovancevic *et al.* 2019, Shariati *et al.* 2019a). Also, the mechanical properties of corroded concrete are reduced compared to the intact concrete. Therefore, the corroded high-performance concrete and reinforced concrete should be investigated under different experimental tests, which lead to evaluating the performance of these concretes after exposure to corrosion effects and determining the design characteristics (Arabnejad Khanouki *et al.* 2010, Jalali *et al.* 2012, Abedini *et al.* 2017, Nosrati *et al.* 2018, Ziaei-Nia *et al.* 2018, Abedini *et al.* 2019, Sajedi *et al.* 2019).

In addition, concrete could be employed in steel-concrete composite. Since the dynamic behavior of the composite systems has always been of interest to researchers, constructions produced from concrete should be investigated under seismic loadings, especially after exposure to corrosion (Daie *et al.* 2011, Kazerani *et al.* 2014, Najarkolaie *et al.* 2017, Zandi *et al.* 2018).

The limitation in the conventional theoretical and experimental methods makes the quest for more cost-effective adaptive and leads to use the easy models that offer effective generalization capability to new data cases. In order to overcome the limitation, computational intelligence techniques are hypothesized to mine the vast and robust experimental data. Artificial Neural Network (ANN) is a commonly used computational intelligence process in different engineering applications (Vanluchene *et al.* 1990, Wu *et al.* 1992, Waszczyszyn *et al.* 2001, Abdalla *et al.* 2007, Shao *et al.* 2015, Shao *et al.* 2018, Shao *et al.* 2019, Shariati *et al.* 2019b, Shariati *et al.* 2019c).

Adaptive Neuro-Fuzzy Inference System (ANFIS) is a type of ANN which is based on the Takagi-Sugeno fuzzy system. This inference system has the potential to capture the solving benefits, for both fuzzy logic and neural network principles, in one framework. Thus, nonlinear functions can be approximated via a set of fuzzy rules of (IF-THEN) (Abraham 2005, Tahmasebi *et al.* 2010, Tahmasebi *et al.* 2012, Toghroli *et al.* 2014, Safa *et al.* 2016, Sedghi *et al.* 2018).

Moreover, the computational intelligence technique is dealing with extracting hidden patterns from historical knowledge to predict unknown future states (Cohen *et al.* 2014). Hence, this technique demonstrates superior accomplishment in analytical processes and regression analyses. ANN has been adopted in many engineering problems with good performance (Sedghi *et al.* 2018). The investigation of strength for corroded reinforced concrete members has not been handled with ANFIS. Accordingly, it is intended to fill this gap of research by proposing new ANFIS model for this application in present work. As a result, an adaptive neuro-fuzzy inference system (ANFIS) (Jang 1993) was used to determine the most dominant 23 input parameters on the nine output factors.

2. Statistical data

The required data for this investigation were collected

Table 2 Output parameters

Output No.	Output Name	Output No.	Output Name
Output 1	f'_c corroded (MPa)	Output 6	f_y corroded (MPa)
Output 2	f_t corroded (MPa)	Output 7	f_u corroded (MPa)
Output 3	E_c corroded (MPa)	Output 8	f'_y corroded (MPa)
Output 4	A_s corroded (mm^2)	Output 9	f'_u corroded (MPa)
Output 5	A'_s corroded (mm^2)		

Table 3 Details of the inputs and outputs

Inputs & Outputs	Minimum	Maximum	Average	Standard deviation
Span length (mm)	900.00	14000.00	2587.94	2858.12
Width (mm)	80.00	2000.00	240.84	431.50
Depth (mm)	140.00	700.00	224.49	123.37
Age (day)	0.00	9490.00	799.06	1979.06
f'_c uncorroded (MPa)	10.70	63.00	33.50	10.93
f_t uncorroded (MPa)	1.85	6.80	3.57	0.80
E_c uncorroded (MPa)	15438.62	300000.00	29606.89	26812.29
P_u corroded (kN)	2.50	650.00	64.27	103.89
Delta corroded (mm)	1.80	200.00	27.62	46.66
A_s uncorroded (mm^2)	78.50	8164.00	700.41	1832.32
A'_s uncorroded (mm^2)	0.00	2260.80	209.18	504.93
Spacing as (mm)	22.00	106.00	55.13	20.37
Spacing A'_s (mm)	0.00	128.00	59.14	31.23
Compressive strain at f'_c uncorroded	2.08E-03	2.49E-03	2.18E-03	3.88E-05
Crushing strain uncorroded	4.09E-03	4.82E-03	4.44E-03	1.23E-04
Tensile strain at f_t uncorroded	1.00E-04	2.00E-04	1.32E-04	1.25E-05
f_y uncorroded (MPa)	345.00	585.00	486.45	84.03
f'_y uncorroded (MPa)	428.00	891.25	677.78	108.85
Number of beams per span	0.00	1.00	0.94	0.23
Number of decks per span	0.00	1.00	0.06	0.23
Number of spans	1.00	3.00	1.26	0.68
f_u uncorroded (MPa)	295.00	626.00	494.01	104.70
f'_u uncorroded (MPa)	428.00	970.30	678.75	131.47
f'_c corroded (MPa)	8.84	63.00	28.84	11.61
f_t corroded (MPa)	1.84	6.80	3.26	0.81
E_c corroded (MPa)	27.53	244430.60	26530.67	22040.57
A_s corroded (mm^2)	61.44	8164.00	648.34	1693.88
A'_s corroded (mm^2)	0.00	2260.80	194.65	467.03
f_y corroded (MPa)	187.82	585.00	458.66	101.31
f_u corroded (MPa)	291.12	891.25	637.36	130.76
f'_y corroded (MPa)	160.60	626.00	457.93	113.81
f'_u corroded (MPa)	248.93	970.30	625.74	131.11

from the literature (Cabrera 1996, Rodriguez *et al.* 1997, Wei-liang and Yu-xi 2001, Shannag and Al-Ateek 2006, Torres-Acosta *et al.* 2007, Vidal *et al.* 2007, Berto *et al.* 2008, Cavaco 2009, Kallias and Rafiq 2010, Castel *et al.* 2011, Khan *et al.* 2011, Oyado *et al.* 2011, Yamamoto *et al.* 2011, Imperatore *et al.* 2012, Khan *et al.* 2012, Zhu and François 2014).

Totally, a dataset containing 107 data points (i.e., the properties of 107 reinforced concrete beams before and after corrosion) was collected. 23 parameters were considered as the inputs of the ANFIS models. Table 1 shows all the input parameters which have the potential to affect the properties of the concrete beams due to corrosion. Output parameters have adopted the properties of the concrete beams after corrosion. These parameters have also been shown in Table 2.

Details of all the input and output parameters are represented in Table 3. As can be seen, the collected data has an excellent frequency, and it also covers an appropriate range of each parameter.

3. ANFIS Methodology

ANFIS is a fuzzy inference system implemented in the framework of adaptive networks. ANFIS network has five layers (Fig. 1). The central core of the ANFIS network is a fuzzy inference system (FIS). The first layer receives inputs (x and y in Fig. 1) and converts them to fuzzy values by membership functions. The rule base contains two fuzzy IF-THEN rules of Takagi and Sugeno's type

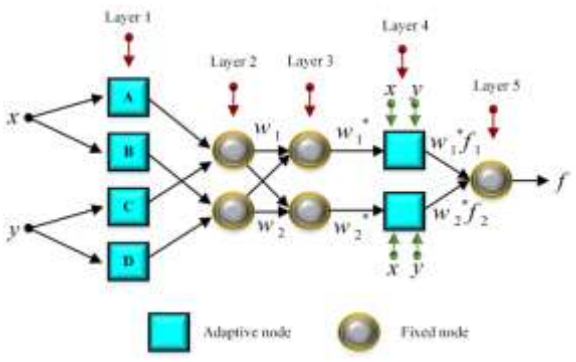

Fig. 1 ANFIS layers

Rule 1: if x is A_1 and y is B_1, then $f_1 = p_1x + q_1y + r_1$,
Rule 2: if x is A_2 and y is B_2, then $f_2 = p_2x + q_2y + r_2$,

Every node in this layer (i.e., the first layer) is selected as an adaptive node with a node function

$$O_i^1 = \mu A_i(x) \tag{1}$$

Where A_i is a linguistic label, and O_i^1 is the membership function of A_i. The bell-shaped membership function is usually selected since it has the highest capacity for the regression of nonlinear data. Bell-shaped membership function with the maximum value of 1 and the minimum value of 0 is defined as follows

$$\mu(x) = bell(x; a_i, b_i, c_i) = \frac{1}{1 + \left[\left(\frac{x-c_i}{a_i}\right)^2\right]^{b_i}} \tag{2}$$

Where $\{a_i, b_i, c_i, d_i\}$ is the parameters set, and x is the input. The parameters of this layer are known as *premise parameters*.

The second layer multiplies the incoming signals and sends their product to the next layer (Fig. 1). For instance

$$w_i = \mu A_i(x) \times \mu B_i(y), \quad i = 1,2. \tag{3}$$

Every output of the nodes exhibits the firing strength of a rule. The third layer is the rule layer. In this layer, the ratio of the i^{th} node firing strength of the rule to those of the other nodes is calculated, which means that

$$w_i^* = \frac{w_i}{w_1 + w_2} \qquad i = 1,2. \tag{4}$$

The outcomes w_i^* are known as normalized firing strength.

The fourth layer is the defuzzification layer in which every node has a node function as follows

$$O_i^4 = w_i^* f_i = w_i^*(p_i x + q_i y + r_i) \tag{5}$$

Where w_i^* is the output of the third layer and $\{p_i, q_i, r_i\}$ are the parameters of this layer known as *consequent parameters*.

The output layer is the 5th layer. In this layer, the overall output is computed by summing all the incoming signals, which means that

$$O_1^5 = f = \sum_i w_i^* f_i \tag{6}$$

In this process, a threshold value between the actual value and the output is set; then, the *consequent parameters* are obtained by the least-squares method, and an error for each data is obtained. If this value is larger than the considered threshold, the premise parameters are updated by the use of a gradient descent method. This process continues until the error becomes less than the threshold. Since the parameters are obtained by two algorithms (i.e., least squares and gradient descent algorithm) simultaneously, the used algorithm in this process is known as a hybrid algorithm.

4. System identification

To identify the most influencing input parameters on each of the outputs, ANFIS models should be developed and trained based on each of the input parameters. As a result, it can be evaluated that how much an input parameter has the potential to be used solely in the prediction of the output. The more precise the ANFIS model can be trained based on that single input, the more influential that input parameter can be. The influence of each input on the output could be evaluated by different statistical indices such as root mean squared error (*RMSE*), coefficient of determination (R^2), and Pearson's correlation coefficient (r). These indices are defined as follows

$$RMSE = \sqrt{\frac{\sum_{k=1}^{S}(P_k - T_k)^2}{S}} \tag{7}$$

$$r = \frac{S\left(\sum_{k=1}^{S} T_k \times P_k\right) - \left(\sum_{k=1}^{S} T_k\right) \times \left(\sum_{k=1}^{S} P_k\right)}{\sqrt{\left(S\sum_{k=1}^{S} T_k^2 - \left(\sum_{k=1}^{S} T_k\right)^2\right) \times \left(S\sum_{k=1}^{S} P_k^2 - \left(\sum_{k=1}^{S} P_k\right)^2\right)}} \tag{8}$$

$$R^2 = \frac{\left[\sum_{k=1}^{S}\left(T_k - \overline{T_k}\right) \cdot \left(P_k - \overline{P_k}\right)\right]^2}{\sum_{k=1}^{S}\left(T_k - \overline{T_k}\right) \cdot \sum_{k=1}^{S}\left(P_k - \overline{P_k}\right)} \tag{9}$$

where P and T are the predicted and target values, and S is the total number of training or testing samples, respectively. Due to the high number of ANFIS models (i.e., 207 models), *RMSE* was only used to identify the most influencing parameters in this study. The low values of *RMSE* show that the ANFIS model is better able to predict the output. Therefore, the input parameter with the lowest value of *RMSE* is the most influencing parameter of the output.

In order to assess the accuracy of the system identification process, 70% of the data were randomly selected for the training phase, and the other 30% was randomly devoted to the testing phase. It is also important to note that all the codes were developed in the MATLAB environment, and its available functions were used.

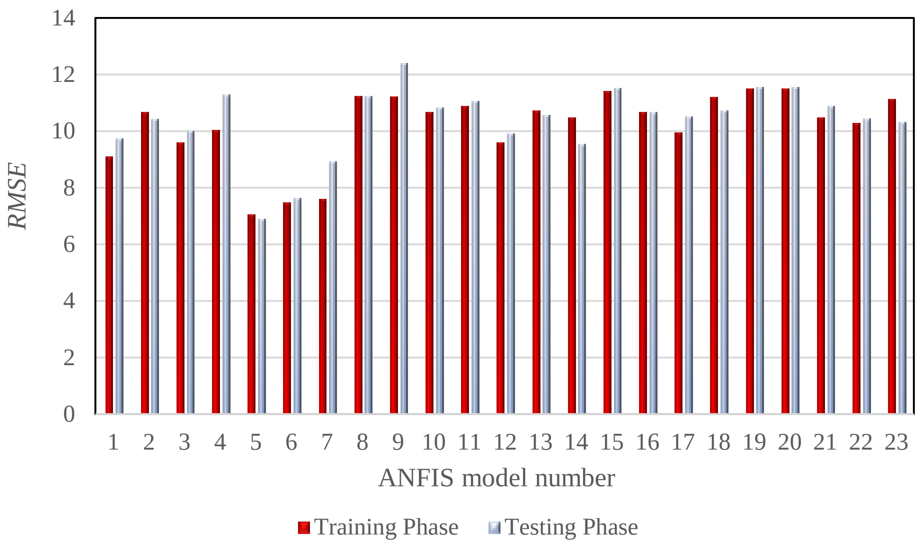

Fig. 2 Testing and training *RMSE* values of the influencing parameters on f'_c

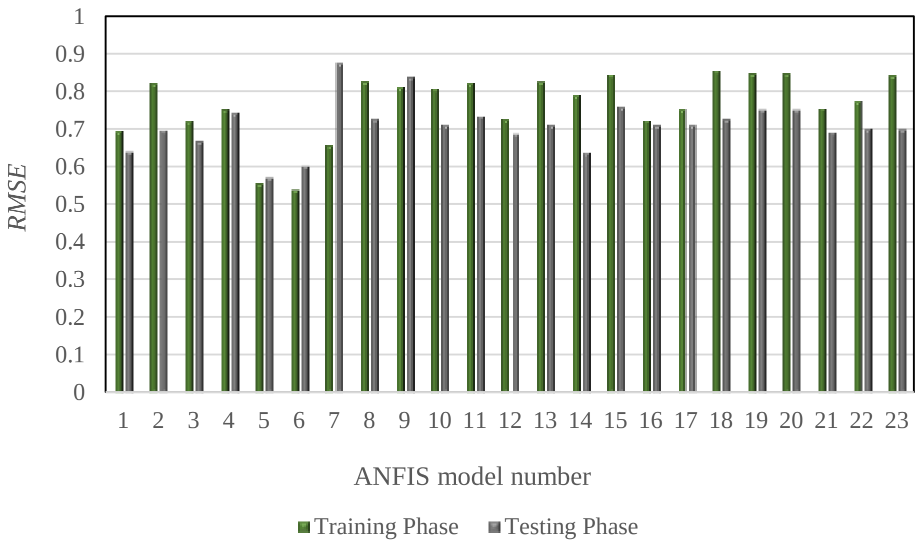

Fig. 3 Testing and training *RMSE* values of the influencing parameters on f_t

5. Results and discussion

Table 4 shows the *RMSE* values in the training and testing phase to predict the corroded compressive strength of concrete (f'_c) as the output. As can be seen, the ability of each input to predict f'_c has been determined in terms of *RMSE*. The lowest value of *RMSE* in the training phase has been obtained for the ANFIS model 5 which means that f'_c uncorroded (input 5) is the most influencing parameter on the f'_c (Output 1) after corrosion.

Fig. 2 demonstrates and compares *RMSE* values in the training and testing phases. It can be observed that in all the models, the value of *RMSE* in the training and testing phase are close to each other. Therefore, it can be concluded that the ANFIS models could predict results accurately and there is not any sign of overfitting or underfitting. This figure also represents that the ANFIS model 5 has the lowest *RMSE* value, and it is the most influencing parameter.

Table 5 illustrates the *RMSE* values in the training and testing phase of ANFIS to predict the corroded tensile strength of concrete (f_t) as the output. As can be realized, the ANFIS model 6 in which uncorroded f_t is the input has the lowest value of *RMSE* in the training phase. Therefore, this parameter is the most influencing parameter on the corroded f_t.

Fig. 3 shows the bar diagram of *RMSE* values in the training and testing phase. The close values of *RMSE* in the testing and training phase confirm the appropriate performance of the developed models. It can be seen in this figure that after the ANFIS model 6, the ANFIS model 5 in

Table 4 *RMSE* values in the testing and training phase (Output= f'_c)

ANFIS model 1: in1 --> Trn =9.1273, Tst=9.7760	ANFIS model 13: in13 --> Trn =10.7523, Tst=10.6083
ANFIS model 2: in2 --> Trn =10.6964, Tst=10.4481	ANFIS model 14: in14 --> Trn =10.5108, Tst=9.5709
ANFIS model 3: in3 --> Trn =9.6270, Tst=10.0312	ANFIS model 15: in15 --> Trn =11.4438, Tst=11.5538
ANFIS model 4: in4 --> Trn =10.0771, Tst=11.3275	ANFIS model 16: in16 --> Trn =10.7010, Tst=10.6975
ANFIS model 5: in5 --> Trn =7.0885, Tst=6.9412	ANFIS model 17: in17 --> Trn =9.9812, Tst=10.5470
ANFIS model 6: in6 --> Trn =7.5136, Tst=7.6768	ANFIS model 18: in18 --> Trn =11.2341, Tst=10.7733
ANFIS model 7: in7 --> Trn =7.6379, Tst=8.9653	ANFIS model 19: in19 --> Trn =11.5371, Tst=11.5941
ANFIS model 8: in8 --> Trn =11.2713, Tst=11.2655	ANFIS model 20: in20 --> Trn =11.5371, Tst=11.5941
ANFIS model 9: in9 --> Trn =11.2534, Tst=12.4362	ANFIS model 21: in21 --> Trn =10.5199, Tst=10.9206
ANFIS model 10: in10 --> Trn =10.7168, Tst=10.8697	ANFIS model 22: in22 --> Trn =10.3128, Tst=10.4844
ANFIS model 11: in11 --> Trn =10.9315, Tst=11.0974	ANFIS model 23: in23 --> Trn =11.1703, Tst=10.3546
ANFIS model 12: in12 --> Trn =9.6410, Tst=9.9516	

* Bold is the best

Table 5 *RMSE* values in the testing and training phase (Output= f_t)

ANFIS model 1: in1 --> Trn =0.6970, Tst=0.6420	ANFIS model 13: in13 --> Trn =0.8278, Tst=0.7131
ANFIS model 2: in2 --> Trn =0.8233, Tst=0.6999	ANFIS model 14: in14 --> Trn =0.7929, Tst=0.6413
ANFIS model 3: in3 --> Trn =0.7234, Tst=0.6693	ANFIS model 15: in15 --> Trn =0.8481, Tst=0.7609
ANFIS model 4: in4 --> Trn =0.7538, Tst=0.7457	ANFIS model 16: in16 --> Trn =0.7244, Tst=0.7127
ANFIS model 5: in5 --> Trn =0.5563, Tst=0.5728	ANFIS model 17: in17 --> Trn =0.7552, Tst=0.7142
ANFIS model 6: in6 --> Trn =0.5406, Tst=0.6045	ANFIS model 18: in18 --> Trn =0.8576, Tst=0.7275
ANFIS model 7: in7 --> Trn =0.6580, Tst=0.8794	ANFIS model 19: in19 --> Trn =0.8493, Tst=0.7535
ANFIS model 8: in8 --> Trn =0.8281, Tst=0.7296	ANFIS model 20: in20 --> Trn =0.8493, Tst=0.7535
ANFIS model 9: in9 --> Trn =0.8144, Tst=0.8394	ANFIS model 21: in21 --> Trn =0.7564, Tst=0.6927
ANFIS model 10: in10 --> Trn =0.8097, Tst=0.7139	ANFIS model 22: in22 --> Trn =0.7776, Tst=0.7031
ANFIS model 11: in11 --> Trn =0.8245, Tst=0.7362	ANFIS model 23: in23 --> Trn =0.8447, Tst=0.7005
ANFIS model 12: in12 --> Trn =0.7281, Tst=0.6893	

* Bold is the best

which uncorroded f'_c is output, can be mentioned as the second most influencing parameter on the corroded f_t.

Table 6 shows that ANFIS model 7 in which uncorroded modulus of elasticity (E_c) is input has the most influence on the corroded E_c having the lowest value of *RMSE* in the training phase.

Fig. 4 shows the *RMSE* values in the testing and training phase. As can be seen in this diagram, although the lowest value of *RMSE* has been obtained for the ANFIS model 7, the ANFIS model 5 and 6 also have low values of *RMSE* which indicate that f'_c and f_t are also influential on the E_c corroded.

RMSE values in the training and testing phase to predict the corroded cross-sectional area of rebar (A_s) is presented in Table 7. As can be seen, the ANFIS model 10, the model in which uncorroded A_s is input, has been able to reach the lower value of *RMSE* in the training phase. Therefore, uncorroded A_s can be represented as the most influential parameter on the corroded A_s.

Fig. 5 shows a comparison of the *RMSE* values obtained from ANFIS models. As can be seen in this figure, some of the ANFIS models have resulted in lower values of *RMSE* compared to other ones, and this shows that corroded A_s has a high dependence on some of the inputs and low dependence on others. According to this figure, inputs of the ANFIS models 1-3, 8-11, and 19-20 highly affect the corroded A_s. However, the inputs of the other ANFIS models are not too influential on the corroded A_s. Table 8 shows the *RMSE* value of the ANFIS models in the training and testing phase to estimate the cross-sectional area of compressive rebar (A'_s). In this table, the ANFIS model 11 in which uncorroded A'_s is input has the greatest influence on the corroded A'_s.

Fig. 6 demonstrates the results of the ANFIS models in a bar diagram. As can be seen, this figure is very similar to Fig. 5. It implies that the same parameters affect the deterioration of the cross-sectional area of both tensile and compressive rebar.

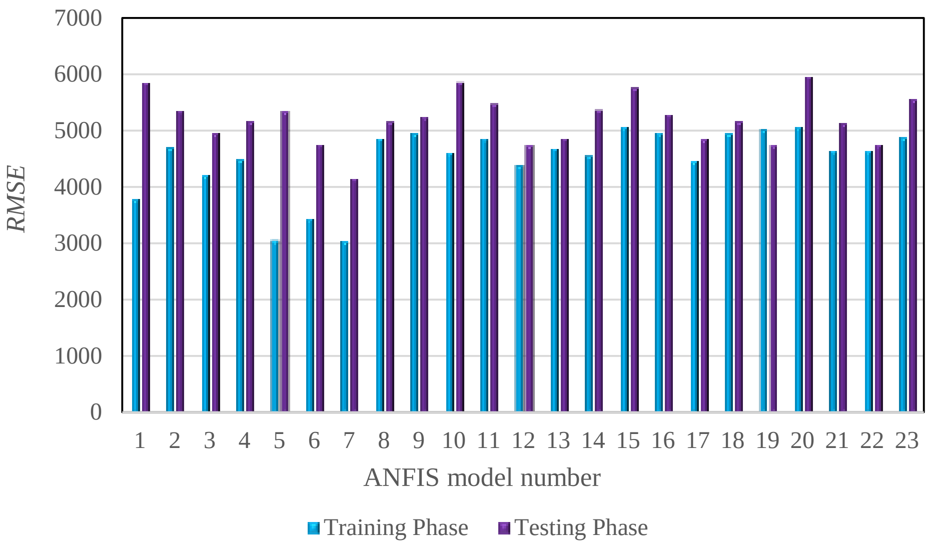

Fig. 4 Testing and training *RMSE* values of the influencing parameters on E_c

Table 6 *RMSE* values in the testing and training phase (Output= E_c)

ANFIS model 1: In1-->Trn=3785.04069, Tst=5863.8867	ANFIS model 13: In13 -->Trn=4686.3211, Tst=4866.1231
ANFIS model 2: In2-->Trn=4696.1355,Tst=5362.5984	ANFIS model 14: In14-->Trn=4555.0939, Tst=5372.5842
ANFIS model 3: In3-->Trn=4221.1628,Tst=4962.0585	ANFIS model 15: In15-->Trn=5070.7578, Tst=5763.8884
ANFIS model 4: In4 -->Trn=4493.4599, Tst=5171.7680	ANFIS model 16: In16-->Trn=4962.2887, Tst=5294.1972
ANFIS model 5: In5-->Trn=3067.8362, Tst=5359.6685	ANFIS model 17: In17-->Trn=4472.9053, Tst=4864.4469
ANFIS model 6: In6-->Trn=3441.8522, Tst=4760.1558	ANFIS model 18: In18 -->Trn= 4954.6503, Tst=5173.6011
ANFIS model 7: In7--> Trn=3050.2301, Tst=4162.0525	ANFIS model 19: In19 -->Trn=5016.2872, Tst=4764.0015
ANFIS model 8: In8--> Trn=4866.5929, Tst=5164.1379	ANFIS model 20: In20 -->Trn=5063.6475, Tst=5964.0015
ANFIS model 9: In9 -->Trn=4952.0184, Tst=5254.5234	ANFIS model 21: In21 -->Trn=4651.8863, Tst=5133.1420
ANFIS model 10: In10-->Trn=4617.9617, Tst=5864.5862	ANFIS model 22: In22-->Trn=4653.8750, Tst=4762.6341
ANFIS model 11: In11 --> Trn=4855.4987, Tst=5480.8328	ANFIS model 23: In23 -->Trn=4886.5794, Tst=5563.5894
ANFIS model 12: In12--> Trn=4377.0689, Tst=4766.0686	

* Bold is the best

These parameters are those in the ANFIS models 1-3, 8-11, and 19-20. Hence, the most influencing parameters on the deterioration of steel rebar include span length, width, depth, P_u corroded, Delta corroded, uncorrded $A_{s,}$ uncorroded A'_s, the number of beams per span, and the number of decks per span.

Presented results in Table 9 reveals that the ANFIS model 17 in which uncorroded f_y is input has the greatest influence on the corroded f_y.

By comparing the *RMSE* values in Fig. 7, it can be concluded that after the uncorroded f_y, the uncorroded ultimate strength of rebar (f_u), i.e., ANFIS model 22 is the most effective parameter on the corroded f_y.

Table 10 shows that the ANFIS model 22 in which uncorroded f_u is input has the strongest relevance for the corroded f_u. The close performance of the ANFIS models in the training and testing phases also confirms the accuracy of the results.

Fig. 8 also shows that after the ANFIS model 22, ANFIS model 17, in which uncorroded f_y is input, exerts the most influence on the output.

Table 11 illustrates that the ANFIS model 18 in which uncorroded f'_y is input has the strongest relevance for the corroded f'_y. The close performance of the ANFIS models in the training and testing phases also confirms the accuracy of the results.

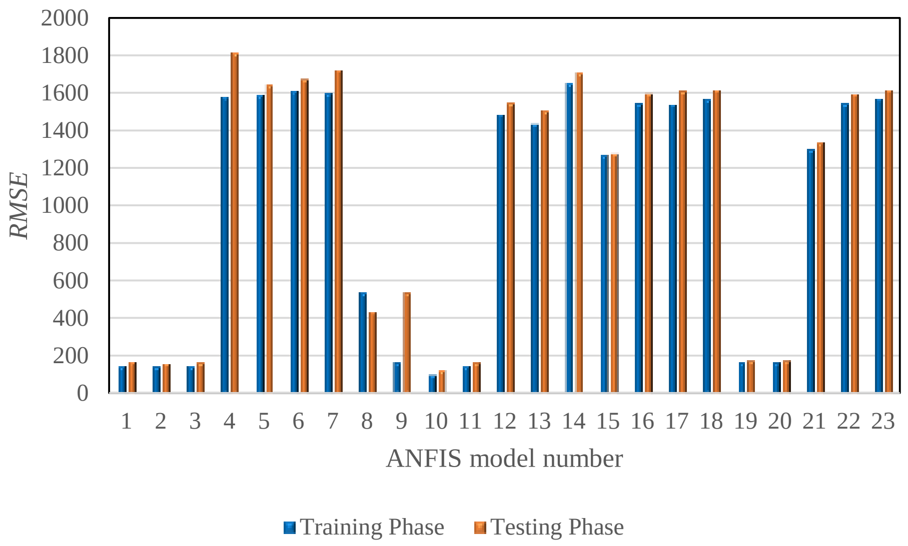

Fig. 5 Testing and training *RMSE* values of the influencing parameters on A_s

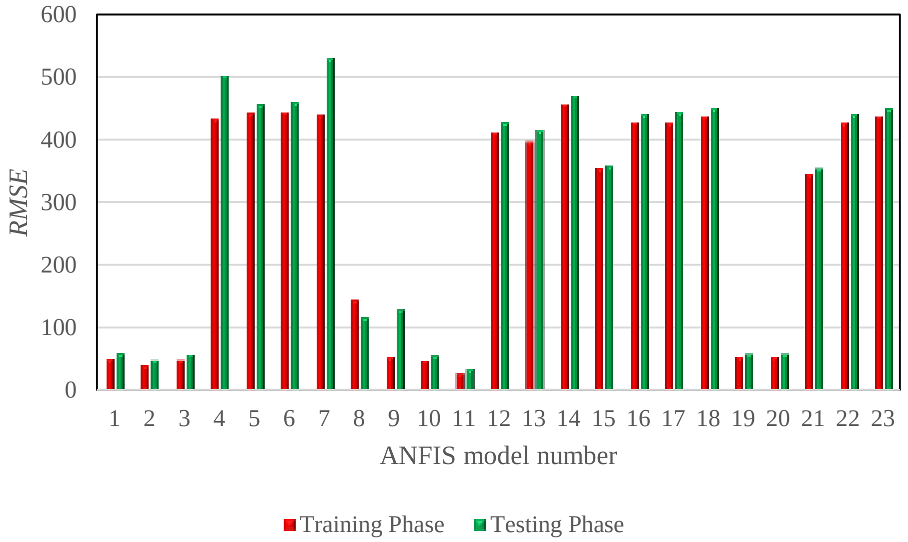

Fig. 6 Testing and training *RMSE* values of the influencing parameters on A'_s

Table 7 *RMSE* values in the testing and training phase (Output=A_s)

ANFIS model 1: in1 --> Trn =150.8687, Tst=173.9192	ANFIS model 13: in13 --> Trn =1438.6543, Tst=1509.3141
ANFIS model 2: in2 --> Trn =147.2872, Tst=164.8105	ANFIS model 14: in14 --> Trn =1658.6530, Tst=1712.1595
ANFIS model 3: in3 --> Trn =149.9399, Tst=169.3641	ANFIS model 15: in15 --> Trn =1272.6686, Tst=1280.7690
ANFIS model 4: in4 --> Trn =1585.9662, Tst=1818.6396	ANFIS model 16: in16 --> Trn =1546.7571, Tst=1598.5660
ANFIS model 5: in5 --> Trn =1595.7391, Tst=1646.0394	ANFIS model 17: in17 --> Trn =1542.4166, Tst=1611.0460
ANFIS model 6: in6 --> Trn =1615.3855, Tst=1674.2866	ANFIS model 18: in18 --> Trn =1570.4355, Tst=1620.2236
ANFIS model 7: in7 --> Trn =1602.7430, Tst=1723.5963	ANFIS model 19: in19 --> Trn =167.0346, Tst=177.5889
ANFIS model 8: in8 --> Trn =542.9044, Tst=438.0014	ANFIS model 20: in20 --> Trn =167.0346, Tst=177.5889
ANFIS model 9: in9 --> Trn =166.6842, Tst=538.3333	ANFIS model 21: in21 --> Trn =1302.7710, Tst=1338.8190
ANFIS model 10: in10 --> Trn =102.1059, Tst=130.9139	ANFIS model 22: in22 --> Trn =1548.4424, Tst=1597.6438
ANFIS model 11: in11 --> Trn =151.0682, Tst=169.2407	ANFIS model 23: in23 --> Trn =1575.1330, Tst=1619.2267
ANFIS model 12: in12 --> Trn =1487.7177, Tst=1549.3569	

* Bold is the best

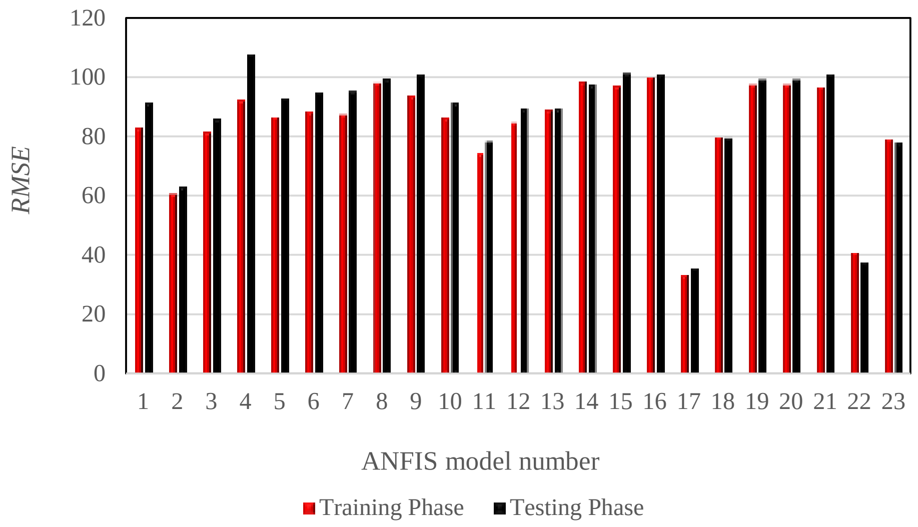

Fig. 7 Testing and training *RMSE* values of the influencing parameters on f_y

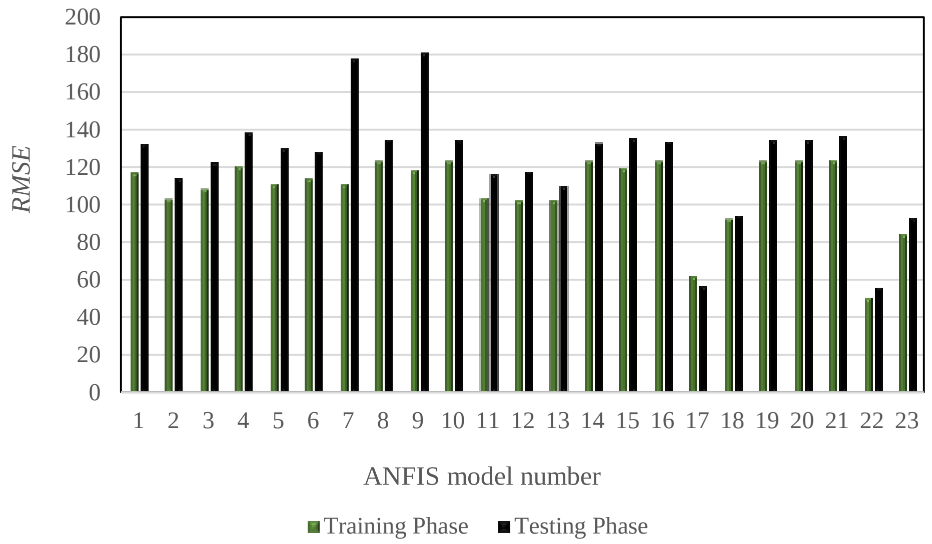

Fig. 8 Testing and training *RMSE* values of the influencing parameters on f_u

Table 8 *RMSE* values in the testing and training phase (Output=A'_s)

ANFIS model 1: in1 --> Trn =51.9402, Tst=60.0758	ANFIS model 13: in13 --> Trn =399.0715, Tst=418.0549
ANFIS model 2: in2 --> Trn =40.8283, Tst=49.4538	ANFIS model 14: in14 --> Trn =457.9679, Tst=471.5092
ANFIS model 3: in3 --> Trn =49.8094, Tst=58.6925	ANFIS model 15: in15 --> Trn =355.9694, Tst=359.0623
ANFIS model 4: in4 --> Trn =435.4460, Tst=503.6620	ANFIS model 16: in16 --> Trn =430.0482, Tst=442.3614
ANFIS model 5: in5 --> Trn =444.0244, Tst=457.3344	ANFIS model 17: in17 --> Trn =428.9259, Tst=446.2820
ANFIS model 6: in6 --> Trn =446.0817, Tst=461.2333	ANFIS model 18: in18 --> Trn =439.5036, Tst=451.9191
ANFIS model 7: in7 --> Trn =440.6131, Tst=531.8665	ANFIS model 19: in19 --> Trn =55.5671, Tst=59.4843
ANFIS model 8: in8 --> Trn =145.1752, Tst=117.0749	ANFIS model 20: in20 --> Trn =55.5671, Tst=59.4843
ANFIS model 9: in9 --> Trn =55.4326, Tst=129.6548	ANFIS model 21: in21 --> Trn =347.4823, Tst=355.0038
ANFIS model 10: in10 --> Trn =48.5208, Tst=56.2669	ANFIS model 22: in22 --> Trn =429.7668, Tst=442.5460
ANFIS model 11: in11 --> Trn =27.5301, Tst=36.0207	ANFIS model 23: in23 --> Trn =439.7008, Tst=450.8545
ANFIS model 12: in12 --> Trn =414.0701, Tst=428.9598	

* Bold is the best

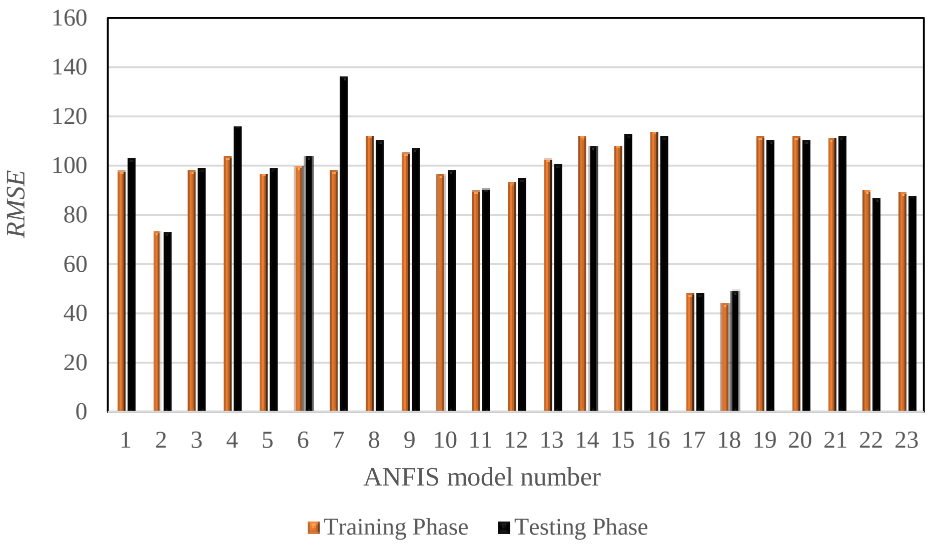

Fig. 9 Testing and training *RMSE* values of the influencing parameters on f'_y

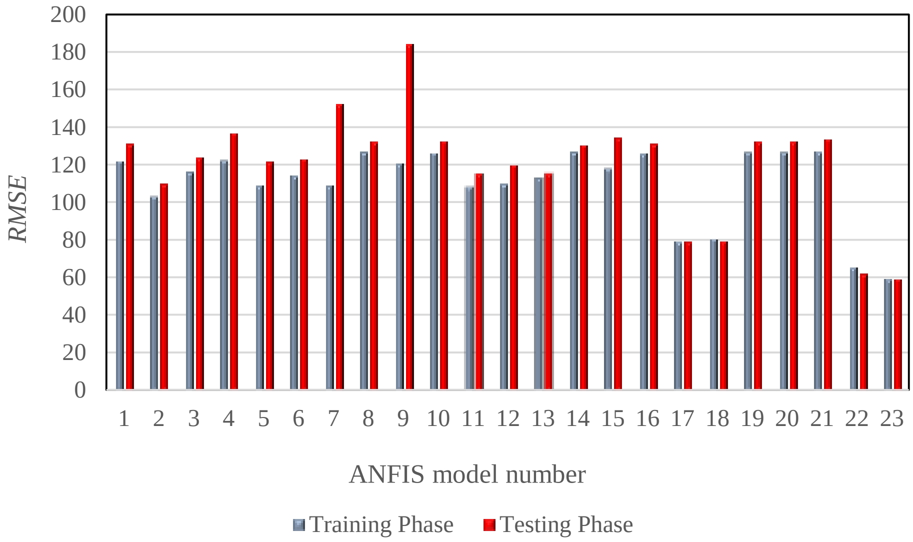

Fig. 10 Testing and training *RMSE* values of the influencing parameters on f'_u

Table 9 *RMSE* values in the testing and training phase (Output=f_y)

ANFIS model 1: in1 --> Trn =83.0242, Tst=91.6387	ANFIS model 13: in13 --> Trn =88.9852, Tst=89.7654
ANFIS model 2: in2 --> Trn =60.7557, Tst=63.3899	ANFIS model 14: in14 --> Trn =98.3258, Tst=97.5788
ANFIS model 3: in3 --> Trn =81.5843, Tst=85.8978	ANFIS model 15: in15 --> Trn =97.1128, Tst=101.3703
ANFIS model 4: in4 --> Trn =92.3948, Tst=107.8825	ANFIS model 16: in16 --> Trn =100.1427, Tst=101.2104
ANFIS model 5: in5 --> Trn =86.8185, Tst=93.0097	**ANFIS model 17: in17 --> Trn =33.5737, Tst=35.9730**
ANFIS model 6: in6 --> Trn =88.6594, Tst=95.0308	ANFIS model 18: in18 --> Trn =80.0712, Tst=79.7636
ANFIS model 7: in7 --> Trn =87.5201, Tst=95.3265	ANFIS model 19: in19 --> Trn =97.5968, Tst=99.3716
ANFIS model 8: in8 --> Trn =98.2366, Tst=99.4456	ANFIS model 20: in20 --> Trn =97.5968, Tst=99.3716
ANFIS model 9: in9 --> Trn =93.8786, Tst=101.1352	ANFIS model 21: in21 --> Trn =96.8406, Tst=101.2988
ANFIS model 10: in10 --> Trn =86.3791, Tst=91.6889	ANFIS model 22: in22 --> Trn =41.2325, Tst=38.0327
ANFIS model 11: in11 --> Trn =74.6219, Tst=78.4736	ANFIS model 23: in23 --> Trn =79.3781, Tst=78.2348
ANFIS model 12: in12 --> Trn =84.8968, Tst=89.3637	

* Bold is the best

Table 10 *RMSE* values in the testing and training phase (Output=f_u)

ANFIS model 1: in1 --> Trn =117.0875, Tst=132.8030	ANFIS model 13: in13 --> Trn =102.4613, Tst=110.4102
ANFIS model 2: in2 --> Trn =103.2499, Tst=114.5027	ANFIS model 14: in14 --> Trn =123.3717, Tst=133.2092
ANFIS model 3: in3 --> Trn =108.6257, Tst=122.7950	ANFIS model 15: in15 --> Trn =119.7251, Tst=135.7573
ANFIS model 4: in4 --> Trn =120.8163, Tst=139.0247	ANFIS model 16: in16 --> Trn =123.3818, Tst=134.0468
ANFIS model 5: in5 --> Trn =111.1402, Tst=130.8203	ANFIS model 17: in17 --> Trn =62.4478, Tst=57.5202
ANFIS model 6: in6 --> Trn =114.1631, Tst=128.6541	ANFIS model 18: in18 --> Trn =92.7095, Tst=94.7566
ANFIS model 7: in7 --> Trn =110.9121, Tst=178.0439	ANFIS model 19: in19 --> Trn =123.3902, Tst=134.9247
ANFIS model 8: in8 --> Trn =123.4068, Tst=135.1266	ANFIS model 20: in20 --> Trn =123.3902, Tst=134.9247
ANFIS model 9: in9 --> Trn =118.6089, Tst=181.4521	ANFIS model 21: in21 --> Trn =124.1062, Tst=136.7171
ANFIS model 10: in10 --> Trn =123.3401, Tst=134.9105	**ANFIS model 22: in22 --> Trn =51.1527, Tst=56.7449**
ANFIS model 11: in11 --> Trn =104.0568, Tst=117.1773	ANFIS model 23: in23 --> Trn =84.9440, Tst=93.6050
ANFIS model 12: in12 --> Trn =102.5639, Tst=118.1226	

* Bold is the best

Table 11 *RMSE* values in the testing and training phase (Output=f'_y)

ANFIS model 1: in1 --> Trn =98.1040, Tst=103.1791	ANFIS model 13: in13 --> Trn =102.9661, Tst=100.7698
ANFIS model 2: in2 --> Trn =73.4324, Tst=73.8889	ANFIS model 14: in14 --> Trn =112.5578, Tst=108.4107
ANFIS model 3: in3 --> Trn =98.4212, Tst=99.0255	ANFIS model 15: in15 --> Trn =108.4927, Tst=112.7859
ANFIS model 4: in4 --> Trn =103.8520, Tst=116.5654	ANFIS model 16: in16 --> Trn =114.0204, Tst=112.2195
ANFIS model 5: in5 --> Trn =97.1787, Tst=99.3722	ANFIS model 17: in17 --> Trn =48.2555, Tst=48.2762
ANFIS model 6: in6 --> Trn =100.5184, Tst=104.3651	**ANFIS model 18: in18 --> Trn =44.3942, Tst=49.7037**
ANFIS model 7: in7 --> Trn =98.3239, Tst=136.6306	ANFIS model 19: in19 --> Trn =111.8574, Tst=110.6067
ANFIS model 8: in8 --> Trn =112.4191, Tst=110.6589	ANFIS model 20: in20 --> Trn =111.8574, Tst=110.6067
ANFIS model 9: in9 --> Trn =105.4211, Tst=107.5298	ANFIS model 21: in21 --> Trn =111.2064, Tst=112.3489
ANFIS model 10: in10 --> Trn =96.5250, Tst=98.6031	ANFIS model 22: in22 --> Trn =90.5911, Tst=87.1705
ANFIS model 11: in11 --> Trn =90.0935, Tst=90.8986	ANFIS model 23: in23 --> Trn =89.7288, Tst=88.2025
ANFIS model 12: in12 --> Trn =93.6944, Tst=95.0069	

* Bold is the best

Fig. 9 also shows that after the ANFIS model 18, ANFIS model 17, in which uncorroded f_y is input, exerts the most influence on the output.

Table 12 shows that the ANFIS model 23 in which uncorroded f'_u is input has the strongest relevance for the corroded f'_u. The close performance of the ANFIS models in the training and testing phases also confirms the accuracy of the results.

Fig. 10 also shows that after the ANFIS model 23, ANFIS model 22, in which uncorroded f_u is input, exerts the most influence on the output.

6. Conclusions

In this study, the most influencing parameters on the corrosion of reinforced concrete beams were investigated. In order to identify the impact of these parameters on the properties of corroded concrete beams, a soft computing approach was employed. For this purpose, an adaptive neuro-fuzzy inference system (ANFIS) was used throughout the investigation. 23 parameters that had the potential to exert far-reaching impact on the corroded concrete beams were selected as the inputs of the ANFIS models. Also, 9 structural parameters that generally undergo severe changes due to corrosion were considered as the outputs of the models. Totally, the numbers of 207 ANFIS models were developed, and the impact of each input parameter on each of the output parameters was evaluated. Results of this investigation can be summarized as follows:

- ANFIS is a practical technique in order to identify the most influencing parameters on the deterioration of the concrete beams. This technique can distinguish the main factors of corrosion and eliminate the need for conducting costly and time-consuming analysis.
- The most influencing factor on the corrosion of each property of reinforced concrete beams is primarily the initial state of that property. In other words, uncorroded properties of concrete beams are the most influencing

factors on the corresponding corroded properties of these beams.

- Although the initial state of each property mainly governs the corrosion of concrete beams, it was found that many other parameters, such as the size of the concrete members, affect the corrosion of the steel rebar. Therefore, these parameters can also be considered in order to control the corrosion of rebar in concrete members.

References

Abdalla, J.A., *et al.* (2007), "Modeling and simulation of shear resistance of R/C beams using artificial neural network", *J. Franklin Institute*, **344**(5), 741-756.

Abedini, M., *et al.* (2017), "Evaluation of concrete structures reinforced with fiber reinforced polymers bars: A review", *J. Asian Scientific Res.*, **7**(5), 165.DOI: 10.18488/journal.2.2017.75.165.175.

Abedini, M., *et al.* (2019), "Large deflection behavior effect in reinforced concrete columns exposed to extreme dynamic loads", engrXiv: 32. DOI: http://dx.doi.org/10.31224/osf.io/6n5fs.

Abraham, A. (2005), Adaptation of fuzzy inference system using neural learning. Fuzzy systems engineering, Springer**:** 53-83.

Altoubat, S., *et al.* (2016), "Laboratory simulation of corrosion damage in reinforced concrete", *Int. J. Concrete Struct. Mater.*, **10**(3), 383.

Arabnejad Khanouki, M.M., *et al.* (2010). "Investigation of seismic behaviour of composite structures with concrete filled square steel tubular (CFSST) column by push-over and time-history analyses", *Proceedings of the 4th International Conference on Steel & Composite Structures*.

Arabnejad Khanouki, M.M., *et al.* (2011), "Behavior of through beam connections composed of CFSST columns and steel beams by finite element studying", *Adv. Mater. Res.*, **168**: 2329-2333. DOI: http://dx.doi.org/10.4028/www.scientific.net/AMR.168-170.2329.

Arabnejad Khanouki, M.M., *et al.* (2016). "Investigation of through beam connection to concrete filled circular steel tube (CFCST) column", *J. Constr. Steel Res.*, **121**, 144-162. DOI: https://doi.org/10.1016/j.jcsr.2016.01.002.

Azad, A.K., *et al.* (2007), "Residual strength of corrosion-damaged reinforced concrete beams", *ACI Mater. J.*, **104**(1), 40.

Berto, L., *et al.* (2008), "Numerical modelling of bond behaviour in RC structures affected by reinforcement corrosion", *Eng. Struct.*, **30**(5), 1375-1385.

Berto, L., *et al.* (2009), "Seismic assessment of existing RC structures affected by degradation phenomena", *Struct. Saf.*, **31**(4), 284-297.

Bossio, A., *et al.* (2017), Evaluation of seismic behavior of corroded reinforced concrete structures", *Proceedings of the 15th International Forum World Heritage and Disaster*, Capri, Italy.

Bossio, A., *et al.* (2018), "An overview of assessment and retrofit of corroded reinforced concrete structures", Procedia Structural Integrity, **11**, 394-401.

Bossio, A., *et al.* (2015), "Modeling of concrete cracking due to corrosion process of reinforcement bars", *Cement Concrete Res.*, **71**, 78-92.

Broomfield, J. (1997), Corrosion of steel in concrete. UK: E & FN Spon, Chapman & Hall.

Cabrera, J. (1996), "Deterioration of concrete due to reinforcement steel corrosion", *Cement Concrete Compos.*, **18**(1), 47-59.

Castel, A., *et al.* (2011), Modelling the stiffness reduction of corroded reinforced concrete beams after cracking. Modelling of Corroding Concrete Structures, Springer**:** 219-230.

Cavaco, E.S. (2009), Robustness of corroded reinforced concrete structures.

Cohen, P., *et al.* (2014), Applied multiple regression/correlation analysis for the behavioral sciences, Psychology Press.

Committee, A. and Standardization, I.O.f. (2008), Building code requirements for structural concrete (ACI 318-08) and commentary, American Concrete Institute.

Coronelli, D. and Gambarova, P. (2004), "Structural assessment of corroded reinforced concrete beams: modeling guidelines", *J. Struct. Eng.*, **130**(8), 1214-1224.

Daie, M., *et al.* (2011), "A new finite element investigation on pre-bent steel strips as damper for vibration control", *Int. J. Phys. Sci.*, **6**(36), 8044-8050. DOI: https://doi.org/10.5897/ijps11.1585.

Davoodnabi, S.M., *et al.* (2019), "Behavior of steel-concrete composite beam using angle shear connectors at fire condition", *Steel Compos. Struct.*, **30**(2), 141-147. DOI: https://doi.org/10.12989/scs.2019.30.2.141.

Fernandez, I. and Berrocal, C.G. (2019), "Mechanical properties of 30 year-old naturally corroded steel reinforcing bars", *Int. J. Concrete Struct. Mater.*, **13**(1), 9.

Hamdia, K.M., *et al.* (2015), "Predicting the fracture toughness of PNCs: A stochastic approach based on ANN and ANFIS", *Comput. Mater. Sci.*, **102**, 304-313. DOI: https://doi.org/10.1016/j.commatsci.2015.02.045.

Hamidian, M., *et al.* (2012), "Application of Schmidt rebound hammer and ultrasonic pulse velocity techniques for structural health monitoring", *Scientific Res. Essays*, **7**(21), 1997-2001. DOI: http://dx.doi.org/10.5897/SRE11.1387.

Heydari, A. and Shariati, M. (2018), "Buckling analysis of tapered BDFGM nano-beam under variable axial compression resting on elastic medium", *Struct. Eng. Mech.*, **66**(6), 737-748. DOI: https://doi.org/10.12989/sem.2018.66.6.737.

Hosseinpour, E., *et al.* (2018), "Direct shear behavior of concrete filled hollow steel tube shear connector for slim-floor steel beams", *Steel Compos. Struct.*, **26**(4), 485-499. DOI: https://doi.org/10.12989/scs.2018.26.4.485.

Huang, R. and Yang, C. (1997), "Condition assessment of reinforced concrete beams relative to reinforcement corrosion", *Cement Concrete Compos.*, **19**(2), 131-137.

Imam, A., *et al.* (2015), "Residual strength of corroded reinforced concrete beams using an adaptive model based on ANN", *Int. J. Concrete Struct. Mater.*, **9**(2), 159-172.

Imam, A. and Azad, A.K. (2016), "Prediction of residual shear strength of corroded reinforced concrete beams", *Int. J. Adv. Struct. Eng.*, **8**(3), 307-318.

Imperatore, S., *et al.* (2012), Mechanical behaviour of corroded rebars in reinforced concrete elements. Mechanics, Models and Methods in Civil Engineering, Springer**:** 207-220.

Ismail, M., et al. (2018). "Strengthening of bolted shear joints in industrialized ferrocement construction." Steel and Composite Structures **28**(6): 681-690.

Jalali, A., *et al.* (2012), "Seismic performance of structures with pre-bent strips as a damper", *Int. J. Phys. Sci.*, **7**(26), 4061-4072.

Jang, J.S. (1993), "ANFIS: adaptive-network-based fuzzy inference system", *IEEE T. Syst. Man, Cy.*, **23**(3), 665-685.

Kallias, A.N. and Rafiq, M.I. (2010), "Finite element investigation of the structural response of corroded RC beams", *Eng. Struct.*, **32**(9), 2984-2994.

Katebi, J., *et al.* (2019), "Developed comparative analysis of metaheuristic optimization algorithms for optimal active control of structures", Engineering with Computers: 1-20.

Kazerani, S., *et al.* (2014), "Seismic behavior of drilled beam section in moment connections", *Numer. Method. Civil Eng.*, **1**(2), 21-28.

Khan, I., *et al.* (2011), Mechanical behavior of long-term corroded reinforced concrete beam. Modelling of Corroding Concrete Structures, Springer**:** 243-258.

Khan, I., *et al.* (2012), "Structural performance of a 26-year-old corroded reinforced concrete beam", *Eur. J. Environ. Civil Eng.*, **16**(3-4), 440-449.

Khorami, M., *et al.* (2017), "Evaluation of the seismic performance of special moment frames using incremental nonlinear dynamic analysis", *Struct. Eng. Mech*., **63**(2), 259-268. DOI: https://doi.org/10.12989/sem.2017.63.2.259.

Khorramian, K., *et al.* (2017), "Numerical analysis of tilted angle shear connectors in steel-concrete composite systems", *Steel Compos. Struct*., **23**(1), 67-85. DOI: https://doi.org/10.12989/scs.2017.23.1.067.

Khorramian, K., *et al.* (2015), "Behavior of tilted angle shear connectors", PLoS One **10**(12), e0144288. DOI: https://doi.org/10.1371/journal.pone.0144288.

Khorramian, K., *et al.* (2016), "Behavior of Tilted Angle Shear Connectors (vol 10, e0144288, 2015)", PLoS One, **11**(2).

Kim, H.R., *et al.* (2016). "Evaluation of bond properties of reinforced concrete with corroded reinforcement by uniaxial tension testing", *Int. J. Concrete Struct. Mater*., **10**(3), 43-52.

Li, D., *et al.* (2019), "Application of polymer, silica-fume and crushed rubber in the production of Pervious concrete", *Smart Struct. Syst*., **23**(2), 207-214. DOI: https://doi.org/10.12989/sss.2019.23.2.207.

Lu, C., *et al.* (2017), "A numerical study on the impact resistant capacity of RC beams with corroded reinforcement", *Procedia Eng*., **210**, 341-348.

Luo, Z., *et al.* (2019), "Computational and experimental analysis of beam to column joints reinforced with CFRP plates", *Steel Compos. Struct.*, **30**(3), 271-280. DOI: http://dx.doi.org/10.12989/scs.2019.30.3.271.

Ma, Y., *et al.* (2014), "Fatigue life prediction for aging RC beams considering corrosive environments", *Eng. Struct*., **79**, 211-221.

Maia, L. and Alves, S. (2017), "Low durability of concrete elements due to steel corrosion–cases wherein the steel reinforcing bars acted as an internal clock bomb", *Procedia Struct. Integrity*, **5**, 139-146.

Mansouri, I., *et al.* (2016). "Strength prediction of rotary brace damper using MLR and MARS", *Struct. Eng. Mech*., **60**(3), 471-488.

Mansouri, I., *et al.* (2019). "Analysis of influential factors for predicting the shear strength of a V-shaped angle shear connector in composite beams using an adaptive neuro-fuzzy technique", *J. Intel. Manufact*., **30**(3), 1247-1257.

Milovancevic, M., *et al.* (2019), "UML diagrams for dynamical monitoring of rail vehicles", *Physica A: Statistical Mechanics and its Applications*, **53**, 121169.

Mohammadhassani, M., *et al.* (2014), "An experimental study on the failure modes of high strength concrete beams with particular references to variation of the tensile reinforcement ratio", *Eng. Fail. Anal*., **41**, 73-80. DOI: https://doi.org/10.1016/j.engfailanal.2013.08.014.

Mohammadhassani, M., *et al.* (2015), "Fuzzy modelling approach for shear strength prediction of RC deep beams", *Smart Struct. Syst*., **16**(3), 497-519. DOI: https://doi.org/10.12989/sss.2015.16.3.497.

Mohammadhassani, M., *et al.* (2014). "Ductility and strength assessment of HSC beams with varying of tensile reinforcement ratios", *Struct. Eng. Mech*., **48**(6), 833-848. DOI: https://doi.org/10.12989/sem.2013.48.6.833.

Mohammed, A., *et al.* (2018), "Simplified finite element model for evaluation of ultimate capacity of corrosion-damaged reinforced concrete beam-columns", *Int. J. Adv. Struct. Eng*., **10**(4), 381-400.

Najarkolaie, K.F., *et al.* (2017), "Realistic behavior of infilled steel frames in seismic events: experimental and analytical study", *Bull. Earthq. Eng.*, **15**(12), 5365-5392.DOI: 10.1007/s10518-017-0173-z.

Nasrollahi, S., *et al.* (2018), "Investigation of pipe shear connectors using push out test", *Steel Compos. Struct*., **27**(5), 537-543. DOI: http://dx.doi.org/10.12989/scs.2018.27.5.537.

Nosrati, A., *et al.* (2018), "Portland cement structure and its major oxides and fineness", *Smart Struct. Syst*., **22**(4), 425-432. DOI: https://doi.org/10.12989/sss.2018.22.4.425.

Ou, Y.C., *et al.* (2012), "Cyclic performance of large-scale corroded reinforced concrete beams", *Earthq. Eng. Struct. D.*, **41**(4), 593-604.

Oyado, M., *et al.* (2011), "Bending performance of reinforced concrete member deteriorated by corrosion", *Struct. Infrastruct. Eng*., **7**(1-2), 121-130.

Paul, S.C. and Van Zijl, G.P.A.G. (2017), "Corrosion deterioration of steel in cracked SHCC", *Int. J. Concrete Struct. Mater.*, **11**(3), 557-572.

Rodriguez, J., *et al.* (1997), "Load carrying capacity of concrete structures with corroded reinforcement", *Constr. Build. Mater.*, **11**(4), 239-248.

Sadeghipour Chahnasir, E., *et al.* (2018), "Application of support vector machine with firefly algorithm for investigation of the factors affecting the shear strength of angle shear connectors", *Smart Struct. Syst.*, **22**(4), 413-424. DOI: http://dx.doi.org/10.12989/sss.2018.22.4.413.

Safa, M., *et al.* (2016), "Potential of adaptive neuro fuzzy inference system for evaluating the factors affecting steel-concrete composite beam's shear strength", *Steel Compos Struct.*, **21**(3), 679-688. DOI: https://doi.org/10.12989/scs.2016.21.3.679.

Sajedi, F. and Shariati, M. (2019), "Behavior study of NC and HSC RCCs confined by GRP casing and CFRP wrapping", *Steel Compos. Struct.*, **30**(5), 417-432. DOI: https://doi.org/10.12989/scs.2019.30.5.417.

Sari, P.A., *et al.* (2018), "An intelligent based-model role to simulate the factor of safe slope by support vector regression", *Eng. Comput*., 1-11.

Sedghi, Y., *et al.* (2018), "Application of ANFIS technique on performance of C and L shaped angle shear connectors", *Smart Struct. Syst.*, **22**(3), 335-340. DOI: https://doi.org/10.12989/sss.2018.22.3.335.

Sen, R., *et al.* (1999), "Durability of carbon fiber-reinforced polymer/epoxy/concrete bond in marine environment", *Struct. J.*, **96**(6), 906-914.

Shah, S., *et al.* (2016), "Behavior of steel pallet rack beam-to-column connections at elevated temperatures", *Thin Wall. Struct*., **106**, 471-483. DOI: https://doi.org/10.1016/j.tws.2016.05.021.

Shahabi, S., *et al.* (2016), "Numerical analysis of channel connectors under fire and a comparison of performance with different types of shear connectors subjected to fire", *Steel Compos. Struct*., **20**(3), 651-669. DOI: https://10.12989/scs.2016.20.3.651.

Shahabi, S., *et al.* (2016), "Performance of shear connectors at elevated temperatures-A review", *Steel Compos. Struct*., **20**(1), 185-203. DOI: https://doi.org/10.12989/scs.2016.20.1.185.

Shannag, M.J. and Al-Ateek, S.A. (2006), "Flexural behavior of strengthened concrete beams with corroding reinforcement", *Constr. Build. Mater*., **20**(9), 834-840.

Shao, Z., *et al.* (2019), "Estimating the Friction Angle of Black Shale Core Specimens with Hybrid-ANN Approaches", Measurement.

Shao, Z. and Vesel, A. (2015). "Modeling the packing coloring problem of graphs", *Appl. Math. Model*., **39**(13), 3588-3595.

Shao, Z., *et al.* (2018). "Kriging Empirical Mode Decomposition via support vector machine learning technique for autonomous operation diagnosing of CHP in microgrid", *Appl. Therm. Eng*., **145**, 58-70.

Shariat, M., *et al.* (2018), "Computational Lagrangian Multiplier Method by using for optimization and sensitivity analysis of rectangular reinforced concrete beams", *Steel Compos. Struct*., **29**(2), 243-256. DOI: https://doi.org/10.12989/scs.2018.29.2.243.

Shariati, A., *et al.* (2012), "Investigation of channel shear connectors for composite concrete and steel T-beam", *Int. J. Phys. Sci*., **7**(11), 1828-1831. DOI: 10.5897/IJPS11.1604.

Shariati, A., *et al.* (2012), "Various types of shear connectors in composite structures: A review", *Int. J. Phys. Sci*., **7**(22), 2876-2890.

Shariati, A., *et al.* (2014), "Experimental assessment of angle shear connectors under monotonic and fully reversed cyclic loading in high strength concrete", *Constr. Build. Mater.*, **52**, 276-283. DOI: http://dx.doi.org/10.1016/j.conbuildmat.2013.11.036.

Shariati, M. (2013), Behaviour of C-shaped Shear Connectors in Stell Concrete Composite Beams, Jabatan Kejuruteraan Awam, Fakulti Kejuruteraan, Universiti Malaya.

Shariati, M., *et al.* (2011), "Assessing the strength of reinforced concrete structures through Ultrasonic Pulse Velocity and Schmidt Rebound Hammer tests", *Scientific Res. Essays*, **6**(1), 213-220.

Shariati, M., *et al.* (2010), "Experimental and analytical study on channel shear connectors in light weight aggregate concrete. *Proceedings of the 4th International Conference on Steel & Composite Structures*, 21 - 23 July, 2010, Sydney, Australia, Research Publishing Services.

Shariati, M., *et al.* (2011). "Experimental and numerical investigations of channel shear connectors in high strength concrete", *Proceedings of the 2011 world congress on advances in structural engineering and mechanics (ASEM'11+)*.

Shariati, M., *et al.* (2015), "Behavior of V-shaped angle shear connectors: experimental and parametric study", *Mater. Struct*., **49**(9), 3909-3926. DOI: 10.1617/s11527-015-0762-8.

Shariati, M., *et al.* (2016), "Comparative performance of channel and angle shear connectors in high strength concrete composites: An experimental study", *Constr. Build. Mater*., **120**, 382-392. DOI: https://doi.org/10.1016/j.conbuildmat.2016.05.102.

Shariati, M., *et al.* (2012), "Behaviour of C-shaped angle shear connectors under monotonic and fully reversed cyclic loading: An experimental study", *Mater. Design*, **41**, 67-73. DOI: https://doi.org/10.1016/j.matdes.2012.04.039.

Shariati, M., *et al.* (2012), "Fatigue energy dissipation and failure analysis of channel shear connector embedded in the lightweight aggregate concrete in composite bridge girders", *Proceedings of the 5th International Conference on Engineering Failure Analysis*, 1-4 July 2012, Hilton Hotel, The Hague, The Netherlands.

Shariati, M., *et al.* (2013), "Comparison of behaviour between channel and angle shear connectors under monotonic and fully reversed cyclic loading", *Constr. Build. Mater*., **38**, 582-593. DOI: https://doi.org/10.1016/j.conbuildmat.2012.07.050.

Shariati, M., *et al.* (2014), "Fatigue energy dissipation and failure analysis of angle shear connectors embedded in high strength concrete", *Eng. Fail. Anal*., **41**, 124-134. DOI: https://doi.org/10.1016/j.engfailanal.2014.02.017.

Shariati, M., *et al.* (2017), "Assessment of stiffened angle shear connector under monotonic and fully reversed cyclic loading", *Proceedings of the 5th International Conference on Advances in Civil, Structural and Mechanical Engineering-CSM 2017*.

Shariati, M., *et al.* (2019), "Application of waste tire rubber aggregate in porous concrete", *Smart Struct. Syst*., **24**(4), 553-566. DOI: https://doi.org/10.12989/sss.2018.22.4.553.

Shariati, M., *et al*. (2019), "Application of a Hybrid Artificial Neural Network-Particle Swarm Optimization (ANN-PSO) Model in Behavior Prediction of Channel Shear Connectors Embedded in Normal and High-Strength Concrete", *Appl. Sciences*, **9**(24), 5534.

Shariati, M., et al. (2019). "Application of Extreme Learning Machine (ELM) and Genetic Programming (GP) to design steel-concrete composite floor systems at elevated temperatures", *Steel Compos. Struct*., **33**(3), 319-332. DOI: https://doi.org/10.12989/scs.2014.33.3.319.

Shariati, M., *et al.* (2019). "Moment-rotation estimation of steel rack connection using extreme learning machine", *Steel Compos. Struct.*, **31**(5), 427-435.DOI: https://doi.org/10.12989/scs.2019.31.5.427.

Shetty, A., *et al.* (2015), "Experimental and numerical investigation on flexural bond strength behavior of corroded NBS RC beam", *Int. J. Adv. Struct. Eng. (IJASE)*, **7**(3), 223-231.

Shi, X., *et al.* (2019), "Viscoelastic analysis of silica nanoparticle-polymer nanocomposites", *Compos. Part B: Eng.*, **158**, 169-178.

Sinaei, H., *et al.* (2011), "Numerical investigation on exterior reinforced concrete Beam-Column joint strengthened by composite fiber reinforced polymer (CFRP)", *Int. J. Phys. Sci*., **6**(28), 6572-6579.

Sinaei, H., *et al.* (2012), "Evaluation of reinforced concrete beam behaviour using finite element analysis by ABAQUS", *Scientific Res. Essays*, **7**(21), 2002-2009.

Song, L., *et al.* (2019), "Experimental and analytical investigation of the fatigue flexural behavior of corroded reinforced concrete beams", *Int. J. Concrete Struct. Mater*., **13**(1), 24.

Tahmasbi, F., *et al.* (2016), "Shear capacity of C-Shaped and L-shaped angle shear connectors", *PLoS One*, **11**(8), e0156989. DOI: https://doi.org/10.1371/journal.pone.0156989.

Tahmasebi, P. and Hezarkhani, A. (2010), "Comparison of optimized neural network with fuzzy logic for ore grade estimation", *Aus. J. Basic Appl. Sci.*, **4**(5), 764-772.

Tahmasebi, P. and Hezarkhani, A. (2012), "A hybrid neural networks-fuzzy logic-genetic algorithm for grade estimation", *Comput. Geosci*., **42**, 18-27.

Tai, V.V., *et al.* (2017). "Modified genetic algorithm-based clustering for probability density functions", *J. Stat. Comput. Simul*., **87**(10), 1964-1979. DOI: https://doi.org/10.1080/00949655.2017.1300663.

Thang, L.D., *et al.* (2016), "A new design approach based on differential evolution algorithm for geometric optimization of magnetorheological brakes", *Smart Mater. Struct*., **25**(12).

Toghroli, A. (2015), Applications of the ANFIS and LR models in the prediction of shear connection in composite beams/Ali Toghroli, University of Malaya.

Toghroli, A., *et al.* (2018), "Evaluation of the parameters affecting the Schmidt rebound hammer reading using ANFIS method", *Comput Concret*, **21**(5), 525-530. DOI: https://doi.org/10.12989/cac.2018.21.5.525.

Toghroli, A., *et al.* (2014), "Prediction of shear capacity of channel shear connectors using the ANFIS model", *Steel Compos. Struct*., **17**(5), 623-639. DOI: https://doi.org/10.12989/scs.2014.17.5.623.

Toghroli, A., *et al.* (2017), "Investigation on composite polymer and silica fume–rubber aggregate pervious concrete", *Proceedings of the 5th International Conference on Advances in Civil, Structural and Mechanical Engineering - CSM 2017*, Zurich, Switzerland.

Toghroli, A., *et al.* (2018), "A review on pavement porous concrete using recycled waste materials", *Smart Struct. Syst*.,

22(4), 433-440. DOI: https://doi.org/10.12989/sss.2018.22.4.433.

Toghroli, A., *et al.* (2016), "Potential of soft computing approach for evaluating the factors affecting the capacity of steel–concrete composite beam", *J. Intel. Manufact*., 1-9. DOI: 10.1007/s10845-016-1217-y.

Torres-Acosta, A.A., *et al.* (2007), "Residual flexure capacity of corroded reinforced concrete beams", *Eng. Struct*., **29**(6), 1145-1152.

Trung, N.T., *et al.* (2019), "Moment-rotation prediction of precast beam-to-column connections using extreme learning machine", STRUCTURAL ENGINEERING AND MECHANICS **70**(5), 639-647. DOI: https://doi.org/10.12989/sem.2019.70.5.639.

Vanluchene, R. and Sun, R. (1990), "Neural networks in structural engineering", *Comput.‐Aided Civil Infrastruct. Eng*., **5**(3), 207-215.

Vidal, T., *et al.* (2007). "Corrosion process and structural performance of a 17 year old reinforced concrete beam stored in chloride environment", *Cement Concrete Res*., **37**(11), 1551-1561.

Wang, X.H. (2008), "Modeling the flexural carrying capacity of corroded RC beam", *J. Shanghai Jiaotong Univ*., *(Science)* **13**(2), 129-135.

Waszczyszyn, Z. and Ziemiański, L. (2001), "Neural networks in mechanics of structures and materials–new results and prospects of applications", *Comput. Struct*., **79**(22-25), 2261-2276.

Wei-liang, J. and Z. Yu-xi (2001), "Effect of corrosion on bond behavior and bending strength of reinforced concrete beams", *J. Zhejiang University-Science*, **2**(3), 298-308.

Wei, X., *et al.* (2018), "Distribution of shear force in perforated shear connectors", *Steel Compos. Struct*., **27**(3), 389-399. DOI: http://dx.doi.org/10.12989/scs.2018.27.3.389.

Wu, X., *et al.* (1992), "Use of neural networks in detection of structural damage", *Comput. Struct*., **42**(4), 649-659.

Xie, Q., *et al.* (2019), "An experimental study on the effect of CFRP on behavior of reinforce concrete beam column connections", *Steel Compos. Struct*., **30**(5), 433-441. DOI: https://doi.org/10.12989/scs.2019.30.5.433.

Xu, C., *et al.* (2019), "Using genetic algorithms method for the paramount design of reinforced concrete structures", *Struct. Eng. Mech*., **71**(5), 503-513. DOI: https://doi.org/10.12989/sem.2019.71.5.503.

Yamamoto, T., *et al.* (2011), Systematic laboratory test on structural performance of corroded reinforced concrete and its utilization in practice. Modelling of Corroding Concrete Structures, Springer**:** 113-124.

Yan, X., *et al.* (2017). "Experimental studies on mechanical properties of corroded steel bars after elevated temperature", *Procedia Eng*., **210**, 622-629.

Zandi, Y., *et al.* (2018), "Computational investigation of the comparative analysis of cylindrical barns subjected to earthquake", *Steel Compos. Struct.*, **28**(4), 439-447. DOI: https://doi.org/10.12989/scs.2018.28.4.439.

Zhou, S., *et al.* (2019), "Degradation behavior of concrete under corrosive coal mine environment", *Int. J. Mining Sci. Technol.*, **29**(2), 307-312.

Zhu, W. and François, R. (2014), "Corrosion of the reinforcement and its influence on the residual structural performance of a 26-year-old corroded RC beam", *Constr. Build. Mater.*, **51**, 461-472.

Ziaei-Nia, A., *et al.* (2018), "Dynamic mix design optimization of high-performance concrete", *Steel Compos. Struct*., **29**(1), 67-75. DOI: https://doi.org/10.12989/scs.2018.29.1.67.

CC